CLINICAL GENETICS An International Journal of Genetics, Molecular and Personalized Medicine

Clin Genet 2012: 81: 272–277
Printed in Singapore. All rights reserved

CLINICAL GENETICS
doi: 10.1111/j.1399-0004.2011.01834.x

Short Report

Rapidly screening variants of uncertain significance in the MAP3K1 gene for phenotypic effects

Loke J, Ostrer H. Rapidly screening variants of uncertain significance in the MAP3K1 gene for phenotypic effects.
Clin Genet 2012: 81: 272–277. © John Wiley & Sons A/S, 2011

DNA sequencing of candidate genes or whole exomes on a diagnostic or investigational basis will yield a plethora of variants of uncertain significance whose potential phenotypic roles cannot be readily demonstrated by prediction programs, SNP databases nor conventional genetic analysis. Many variants may produce phenotypic changes in the encoded proteins by affecting the quantity, post-translational modification or protein interactions. Here, we establish the application of the method of flow cytometry following immunoprecipitation to show that known protein interactions are altered in the B-lymphoblastoid cells of patients with 46,XY gonadal dysgenesis arising from mutations in the MAP3K1 gene. This method can be scaled readily to test multiple interactions for many variants simultaneously from available tissues as well as quantify the effects of variants on protein accumulation and post-translational modification, thus providing an efficient means for screening variants of uncertain significance for phenotypic effects.

Conflict of interest

There is no conflict of interest to declare.

J Loke[a] and H Ostrer[a,b]

[a]Department of Pathology, and
[b]Department of Genetics, Albert Einstein College of Medicine, Bronx, NY, USA

Key words: disorders of sex development – flow cytometry – MAP kinases – variants of uncertain significance – Western blots

Corresponding author: Harry Ostrer, MD, Departments of Pathology and Genetics, Albert Einstein College of Medicine, 1300 Morris Park Avenue, Ullman 715, Bronx, NY 10461, USA.
Tel.: +1 718 430 8605;
fax: +1 718 430 8541;
e-mail: harry.ostrer@einstein.yu.edu

Received 9 November 2011, revised and accepted for publication 12 December 2011

The availability of accurate, relatively low-cost sequencing methods to analyze the exome or whole genome for novel, rare variants that affect phenotypes has become a game changer in clinical genetics (1). Deciphering the variant data output is not a simple task. For any individual genome, up to 3.5 million single-nucleotide variants and 600,000 indels may be identified (2). Similarly for any given exome, up to 17,000 variants may be identified (3). To reduce the complexity of analysis, variants are filtered for rarity by comparison with catalogs, such as dbSNP and 1000 genomes (3–4). Yet, observing a hit in these catalogs does not negate a possible phenotypic effect. Computational methods, such as NNSPLICE that predicts splicing alteration (5), and SIFT, SNAP and PolyPhen that predict possible deleterious effects based on conservation of encoded amino acids may also fall short for both sensitivity and specificity (6–8). Linkage, homozygosity mapping and other purely genetic methods may lack statistical power from limited number of affected ones within a pedigree or community available for study. Furthermore, demonstration of linkage even at a very high LOD score does not preclude the presence of a second variant in linkage disequilibrium that is in fact causal.

The observation that 85% of previously identified causal variants for monogenic disorders were identified in exons or at splice junction boundaries in introns suggests that the vast majority affect the quantity and/or function of the encoded gene RNA and/or protein products (9). In addition, most proteins are members of multimeric complexes (10). Thus, mutations in a candidate gene may change the quantity of the protein that it encodes, may alter the post-translational modification of that protein or may affect its interaction with its binding partners altogether. All three of these alterations can be assessed by immunoassays, which have been a mainstay for quantifying unmodified and modified proteins for over 30 years (11). These

methods include both immunohistochemical studies of cells and Western blots of cell homogenates. Dual immunoassays, such as those provide by co-immunoprecipitation (co-IP) followed by Western blots have become important for quantifying protein–protein interactions as functional studies (12).

Recently, it has been shown that the dynamic range of co-IP Western blots can be improved by flow cytometry, a direct counting function (13). Using this method, immunoprecipitating antibodies, known as 'bait', are coupled covalently to polystyrene beads whose low autofluorescence is suitable for flow cytometry detection (Fig. 1). Once coupled, the antibodies on beads will immunoprecipitate a specific protein complex in cell lysates. These complexes can then be probed with various fluorescently tagged secondary antibodies to quantify the binding of the interacting partners by counting the bound beads on a flow cytometer.

Here, we have applied this method to probe wild-type B-lymphoblastoid cell lines or those derived from patients with MAP3K1 mutations who have 46,XY gonadal dysgenesis (14). We show that altered binding of interacting proteins that could influence the downstream signaling in testis or ovarian-determining pathways. Because B cell lines express a large repertoire of protein complexes and can be derived from patients with presumed genetic disorders, they represent a readily available resource for screening variants of uncertain phenotypic significance.

Methods

Cell culture and reagents

Three MAP3K1 mutation-bearing Epstein-Barr virus B-lymphoblastoid cells lines (c.634-8A, p.Leu189Arg, and p.Leu189Pro) from individuals with 46,XY complete gonadal dysgenesis and a wild-type cell line were derived, as described previously (14). These cell lines were grown in RPMI medium (Invitrogen A2780, Carlsbad, CA), supplemented with 15%

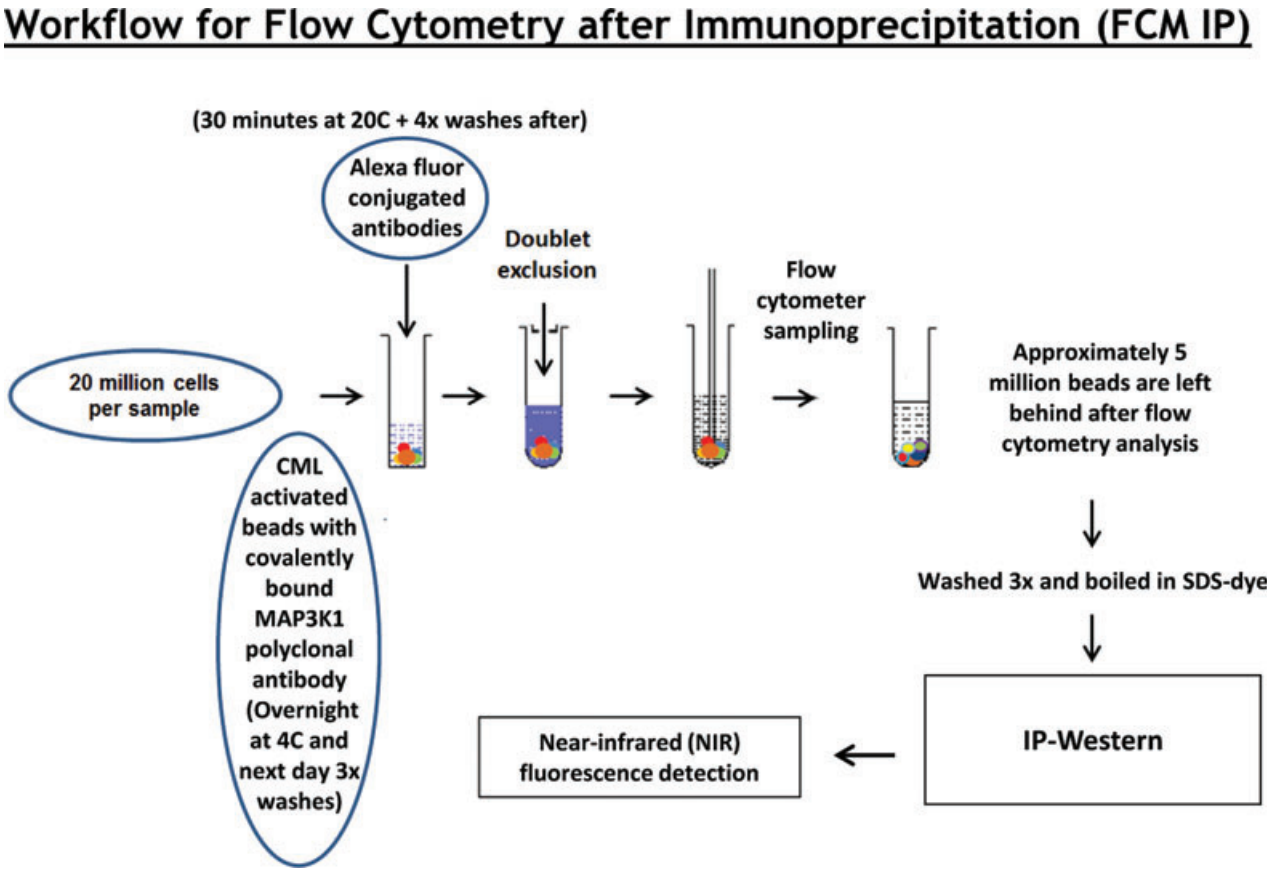

Fig. 1. Workflow for flow cytometry after co-immunoprecipitation. The method was performed according to the described protocol by lysing 20 million human B-lymphoblastoid cells in radio-immunoprecipitation assay (RIPA) lysis buffer with inhibitors. The MAP3K1 multiprotein complex was immunoprecipitated with carboxy-modified polystyrene latex (CML) beads coupled with either MAP3K1 or RHOA rabbit polyclonal antibodies. Alexa-conjugated antibodies of target-binding proteins were added prior to flow cytometric analysis. MAP3K1 or RHOA antibodies were covalently coupled to CML beads for immunoprecipitation. These beads were washed three times in IP buffer prior to incubation with cell lysates. The scatter profile was calibrated to homogeneous beads to avoid detection of the doublet population. Approximately 5–7 million beads were reserved for conventional IP Western blot analysis. These beads were boiled for 10 min at 95°C in 25 µl of sodium dodecyl sulfate loading dye. Then, each sample was loaded on 4–12% gradient Bis–Tris gel and run for 50 min prior to transfer to nitrocellulose membranes. These were probed with the target antibodies, then with infrared (IR) dye-conjugated secondary antibodies. The Licor Odyssey gel scanner was used for detection.

(v/v) fetal bovine serum (FBS) Defined Grade, 50 units/ml penicillin, and 50 g/ml streptomycin at 37°C with 5% CO_2. The antibodies included MAP3K1 rabbit polyclonal antibody (Lifetech #51-340, Carlsbad, CA), RHOA rabbit polyclonal antibody (Abcam #ab66124, Cambridge, MA), MAP3K4 mouse monoclonal (Abcam #55669), IRDye 800CW Goat anti-Mouse (Licor #926-32210, Lincoln, Nebraska), and IRDye 680LT Goat anti-Rabbit IgG (Licor #926-68021). Western blotting analysis was performed as described previously (14).

FCM IP on cultured lymphoblastoid cells

Flow cytometry following immunoprecipitation (FCM IP) was performed, as described previously (13), with the following modifications optimized for lymphoblastoid cell lysates. The bait antibody was conjugated onto carboxyl-modified latex (CML) beads at concentrations of 30 μg/mg of 5 μ CML beads using an antibody coupling kit (Dynal #143.11D, Carlsbad, CA). The protease and phosphatase inhibitors at 4× concentration were added to the cell lysates. Antibody-conjugated CML beads were added to the lysates to incubate overnight at 4°C, rather than 1 h as suggested previously. Alexa 488 and 647 dyes were coupled to the secondary antibodies using labeling kits (Lifetech #A20181 and A20186, respectively). The secondary antibodies were added to the lysate the next day after three to four washes and were incubated at 20°C for 30 min with four additional washes following to reduce the background. Flow cytometry was performed on a BD Excalibur with 96-well, high-throughput capabilities. The counting of bead fluorescence occurrences, 'events', was reduced to 2500 gated events setting from the standard 10,000–20,000 events (13). Note that 'gating' refers to the combination of fluorescence and scatter values that are counted.

Results

The intrinsic fluorescence of the CML beads was low and did not interfere with subsequent analysis of binding fluorochromes (Fig. S1a). The fluorescence of the Alexa 488 and 647 dyes on antibody-conjugated CML beads was used as reference control for calibrating the flow cytometer gate sensor to exclude background noise and to gauge dye detection fidelity (Fig. S1b,c). Positive controls from binding of either MAP3K1 or RHOA complexes to the beads could, in turn, be recognized by the labeled MAP3K1 and RHOA antibodies – showing the specificity of these IP pull-down reactions (Fig. S1d,e). We confirmed by Western blot that the expression of wild-type and mutant MAP3K1 proteins and that the input amounts of MAP3K1 prior to IP were consistent (Figs 2c and S2a). Previously, we showed by Western blot that the input amounts of RHOA prior to IP were consistent (14). The IP Western from the MAP3K1 pull-down of MAP3K4, and the RHOA pull-down of MAP3K1 in the aggregate showed dramatic increases in binding among mutant samples as quantified by densitometry analysis using Licor software 3.0 (Fig. S2b,c).

When applied to the analysis of the patient and control samples to measure protein *interactions*, the binding of MAP3K4 was shown by FCM IP to be increased threefold in these cell lines that contain any of the three endogenous mutant MAP3K1 genes (C.654-8A, p.Leu189Pro and p.Leu189Arg) compared to wild-type cell lines (Figs 2 and S1g–i). The results observed with FCM IP were confirmed by conventional IP Western blots of samples eluted from the CML beads, although the binding appeared to be increased twofold on an average among all mutants. Accordingly, we confirmed that the increases were not the result of unequal loading nor increased expression of MAP3K1 using actin as loading control and MAP3K1 input prior to IP (Fig. S2b).

These methods could also be applied to the *reverse IP* method in which the 'bait' was RHOA, a MAP3K1-interacting protein, and binding of wild-type or mutant MAP3K1 was measured by flow cytometry (Figs 3 and S1k–m). In this case, the binding of the mutant MAP3K1 proteins was increased twofold to fourfold in cells containing mutant compared to wild-type MAP3K1. The results observed with FCM IP were confirmed by conventional IP Western blots of samples eluted from the CML beads, although the binding from all mutant cells appeared to be increased 2.5-fold compared to wild type (Figs 3c and S2c). This discordance may be accounted for by the limited dynamic range of conventional Western blots compared to flow cytometry.

Discussion

Here, we have shown that the effects of missense and in-frame splicing (with insertion of 2 amino acids) mutations in the amino third of the MAP3K1 gene result in increased binding of MAP3K4. This might arise through interactions with their shared binding partner, Axin1 (15, 16). Both MAP kinases compete for Axin binding, albeit at different sites (15), and the presence of these MAP3K1 mutations may alleviate this competition. Unlike MAP3K1, MAP3K4 is an essential testis-determining gene. Homozygous loss of function alleles in mouse Map3k4 lead to disrupted testis development in mice from failure to support cord development (17), whereas knockout of the mouse Map3k1 gene does not (18). Reduction of MAP3K4 protein either from genetic knockout or from sequestration in MAP3K1–MAP3K4 complexes may have functionally similar effects. Increased binding of MAP3K4 to MAP3K1 complexes or knockout of MAP3K4 may affect downstream WNT targets through Axin1. Confirmation will require reporter-based assays. Axin1, an inhibitor of the WNT signaling pathway, interacts with β-catenin to reduce its protein abundance (16, 19). This results in an increase and/or stabilization of β-catenin, an effect that is known to cause male-to-female sex reversal in the XY gonad – in part by reducing SOX9 expression (20).

We have also shown that MAP3K1 from all three mutant MAP3K1 cell lines has enhanced binding to

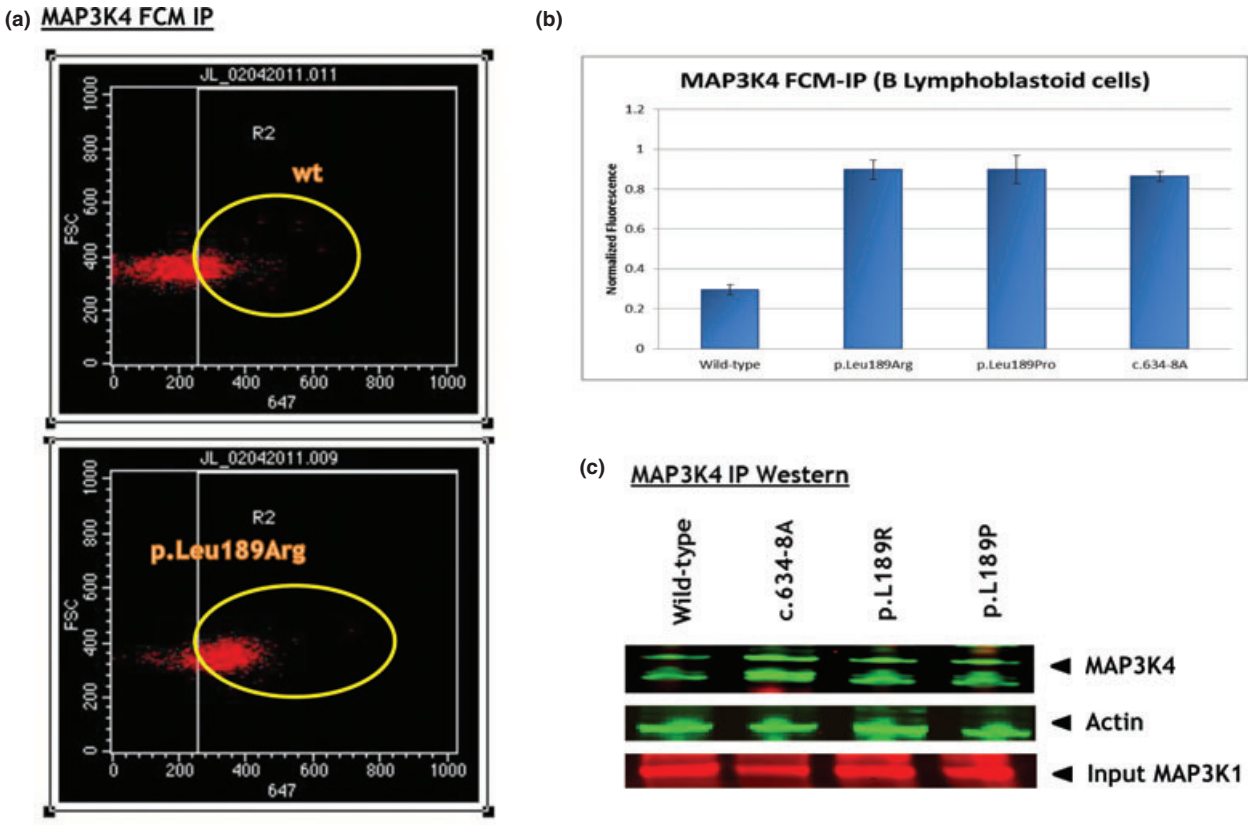

Fig. 2. Flow cytometry following immunoprecipitation was performed on B-lymphoblastoid cells from wild type and p.Leu189Arg using the MAP3K1 bait antibody and the Alexa 647 and Alexa 488-labeled MAP3K4 target antibodies. (**a**) The flow cytometry-gated results show increased binding of MAP3K4 to mutant MAP3K1. (**b**) Results compiled from three independent experiments for each pathogenic mutation, Leu189Arg, p.Leu189Pro and c.634-8A, show increased MAP3K4 binding to mutant MAP3K1 ($p < 0.05$). (**c**) Conventional IP Western blots of primary B-lymphoblastoid cells detect an approximate twofold increase of binding of MAP3K4 to MAP3K1 from all three mutant cell lines compared to wild type. Loading control is actin and input control MAP3K1 on the lowest panel.

RHOA, compared to wild type. RHOA is known to positively regulate MAP3K1 kinase activity by binding to its N-terminal third (21). Previous studies in chondrocytes have shown that the transcriptional activity of SOX9 is regulated by the MAP3K1-binding partner, RHOA (22–24), and that the increase in SOX9 levels in chondrocytes induced by FGF2 is mediated via the MAP kinase pathway (25). Thus, mutations in the MAP3K1 gene family could mediate the balance between the male and female sex-determining pathways by diminishing the activities of the testis-promoting SOX9 and FGF9 genes and increasing the activities of the ovarian-promoting WNT4 and CTNNB1 (β-catenin) genes reviewed in Ref. (26). Such explanations do not require sexually dimorphic expression of MAPK signaling components during gonadogenesis, because transcription of SOX9, FGF9 and WNT4 is already sexually dimorphic. Thus, the 46,XY disorder of gonad development that is associated with mutations in MAP3K1 may be caused by decreased SOX9 activity, increased β-catenin activity, or both.

These approaches of flow cytometry immunoassays, either with or without immunoprecipitation, can be adapted to study other candidate genes with variants of uncertain significance. In the process, they can test the general effects that a variant might have for a protein and its downstream targets: alteration of the accumulation of the protein and the measured quantity in the cell, alteration of the post-translational modification of the protein, such as phosphorylation, or alteration of the interaction of the protein with its cofactors. Typically any or all of these are tested by biological assays to show that a newly identified variant is a mutation, i.e. has a phenotypic effect. Previously it has been shown that the effects on accumulation and post-translational modification can be measured reliably by flow cytometry (13, 27). Here, we have tested and modified a tool that can be used for high-throughput screening of the effects of genetic variants on binding of partners that can be adapted for a 96- or 384-well approach. Thus, multiple variants and multiple-binding partners can be tested in a single experiment. Moreover, comparison of previous IP Western densitometry results with FCM IP shows a greater sensitivity, using only one-fifth the amount of protein required for traditional methods. The multiple-binding partners can be tested in the same tube, because up to 17 antibodies labeled with different fluorochromes with different emission wavelengths can be used simultaneously (27). Furthermore, the method can test not only interactions with binding

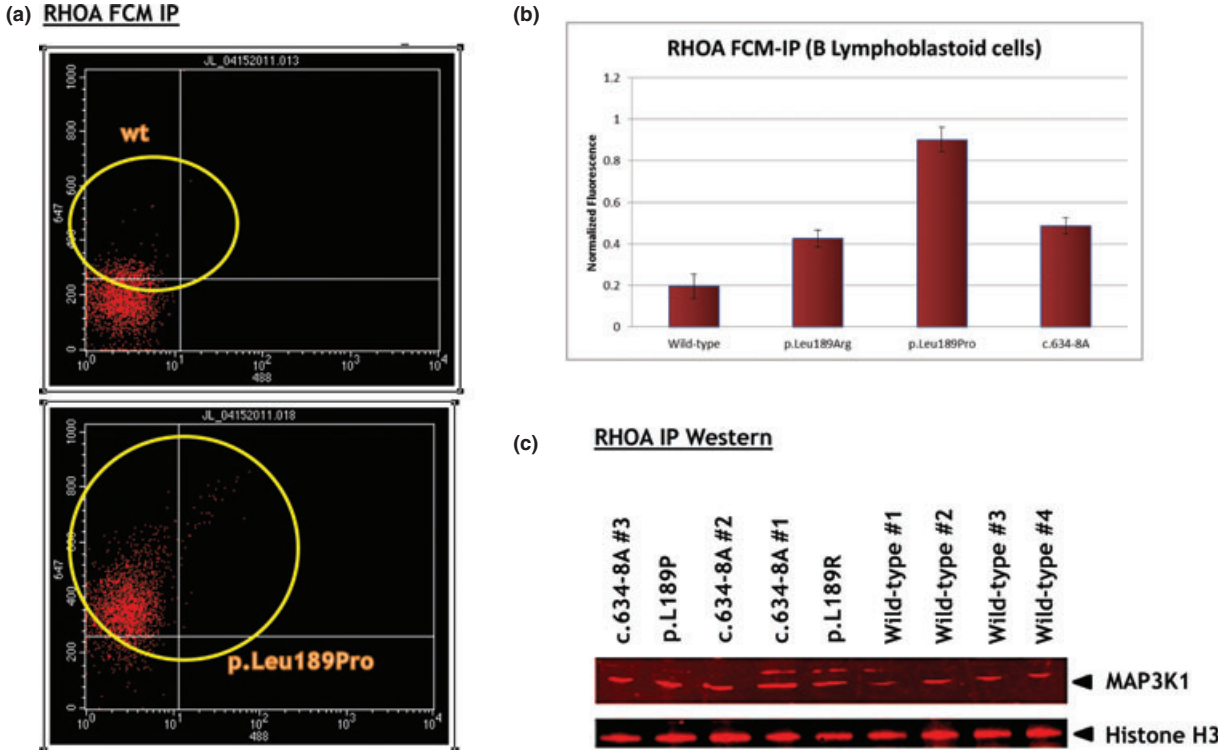

Fig. 3. Reverse flow cytometry following immunoprecipitation performed on B-lymphoblastoid cells from wild type and p.Leu189Arg using the RHOA bait antibody and the Alexa 488-labeled MAP3K1 target antibody. (**a**) The flow cytometry-gated results show increased binding of mutant MAP3K1 to RHOA complexes. (**b**) Results compiled from three independent experiments for each pathogenic mutation, Leu189Arg, p.Leu189Pro and c.634-8A, show increased mutant MAP3K1 binding to RHOA ($p < 0.05$). (**c**) Conventional immunoprecipitation Western blots of primary B-lymphoblastoid cells detect an approximate 2.5-fold increase of binding of mutant MAP3K1 to RHOA from all three mutant cell lines compared to wild type.

partner, but also the quantification of the bound protein itself and its post-translationally modified forms, such as the phosphorylation status of the MAP kinase (28). Although B-lymphoblastoid cells may not be the primary cell type in which the phenotype of the mutant gene is manifested, the gene in question and its multitude of binding partners are commonly expressed in B cells, making protein quantification and quantitative interaction assays possible. Thus, this method may lend itself to testing virtually any variant that is identified by massively parallel-sequencing methods.

Supporting Information

The following Supporting information is available for this article:

Fig. S1. Generation of FCM IP (flow cytometry following immunoprecipitation) raw data for carboxyl-modified latex (CML) bead controls and wild-type and mutant samples. Controls: (**a**) intrinsic fluorescence of a homogeneous population of untreated CML beads. Covalent coupled of IP antibodies to CML beads. (**b**) Alexa 488 dye on antibody-conjugated CML beads used as a reference setting to gate Alexa 488 beam scattering (13). (**c**) Alexa 647 dye on antibody-conjugated CML beads used as a reference setting to gate Alexa 647 beam scattering (13). (**d**) Positive control gating of FCM IP pull-down samples with bait MAP3K1 and target MAP3K1 conjugated Alexa 488 antibody in order to visualize the efficacy of the IP pull-down. (**e**) Gating of FCM IP pull-down samples with bait RHOA and target RHOA in order to visualize the efficacy of the IP pull-down. Samples were treated with MAP3K1-conjugated CML beads and were probed with Alexa 488 and 647-conjugated MAP3K4 antibody, then gated. (**f**) wild type (WT), (**g**) c.634-8, (**h**) p.Leu189Arg, and (**i**) p.Leu189Pro (quantification in Fig. 2b). Samples were treated with RHOA-conjugated CML beads and were probed with Alexa 488-conjugated MAP3K1 antibody then gated. (**j**) WT, (**k**) c.634-8, (**l**) p.Leu189Arg and (**m**) p.Leu189Pro (quantification in Fig. 3b).

Fig. S2. (**a**) Individual sample intensities of MAP3K1 input prior to pull-down for MAP3K4 for Fig. 2c were quantified from conventional Western blots using the LICOR software 3.0. (**b**) After controlling for MAP3K1 loading the intensities were further normalized to actin, showing an average twofold increase of MAP3K4 binding in all mutant samples. (**c**) Reverse IP using RHOA as bait shows increased binding of MAP3K1 to all mutant samples, about 2.5-fold increase compared to WT samples. These results were normalized to histone as a loading control.

Additional Supporting information may be found in the online version of this article.

Please note: Wiley-Blackwell Publishing is not responsible for the content or functionality of any supplementary materials supplied by the authors. Any queries (other than missing material) should be directed to the corresponding author for the article.

References

1. Ostrer H. Changing the game with whole exome sequencing. Clin Genet 2011: 80: 101–103.
2. Pelak K, Shianna KV, Ge D et al. The characterization of twenty sequenced human genomes. PLoS Genet 2010: 6.

3. Ng SB, Turner EH, Robertson PD et al. Targeted capture and massively parallel sequencing of 12 human exomes. Nature 2009: 461: 272–276.
4. Sherry ST, Ward MH, Kholodov M et al. dbSNP: the NCBI database of genetic variation. Nucleic Acids Res 2001: 29: 308–311.
5. Reese MG, Eeckman FH, Kulp D et al. Improved splice site detection in Genie. J Comput Biol 1997: 4: 311–323.
6. Ng PC, Henikoff S. SIFT: predicting amino acid changes that affect protein function. Nucleic Acids Res 2003: 31: 3812–3814.
7. Bromberg Y, Yachdav G, Rost B. SNAP predicts effect of mutations on protein function. Bioinformatics 2008: 24: 2397–2398.
8. Adzhubei IA, Schmidt S, Peshkin L et al. A method and server for predicting damaging missense mutations. Nat Methods 2010: 7: 248–249.
9. Cooper DN, Krawczak M. The mutational spectrum of single base-pair substitutions causing human genetic disease: patterns and predictions. Hum Genet 1990: 85: 55–74.
10. Hartwell LH, Hopfield JJ, Leibler S et al. From molecular to modular cell biology. Nature 1999: 402: C47–C52.
11. Wu AH. A selected history and future of immunoassay development and applications in clinical chemistry. Clin Chim Acta 2006: 369: 119–124.
12. Identification of associated proteins by coimmunoprecipitation. Nat Methods 2005: 2: 475–476.
13. Schrum AG. Visualization of multiprotein complexes by flow cytometry. In: Coligan JE, Bierer BE, Margulies DH, Shevach EM, Strober W, eds. *Current protocols in immunology*, John Wiley & Sons, Somerset, NJ, chapter 5, Unit 5.9.2009.
14. Pearlman A, Loke J, Le Caignec C et al. Mutations in MAP3K1 cause 46,XY disorders of sex development and implicate a common signal transduction pathway in human testis determination. Am J Hum Genet 2010: 87: 898–904.
15. Luo W, Ng WW, Jin LH et al. Axin utilizes distinct regions for competitive MEKK1 and MEKK4 binding and JNK activation. J Biol Chem 2003: 278: 37451–37458.
16. Sue Ng S, Mahmoudi T, Li VS et al. MAP3K1 functionally interacts with Axin1 in the canonical Wnt signalling pathway. Biol Chem 2010: 391: 171–180.
17. Bogani D, Siggers P, Brixey R et al. Loss of mitogen-activated protein kinase kinase kinase 4 (MAP3K4) reveals a requirement for MAPK signalling in mouse sex determination. PLoS Biol 2009: 7: e1000196.
18. Warr N, Bogani D, Siggers P et al. Minor abnormalities of testis development in mice lacking the gene encoding the MAPK signalling component, MAP3K1. PLoS One 2011: 6: e19572.
19. Nakamura T, Hamada F, Ishidate T et al. Axin, an inhibitor of the Wnt signalling pathway, interacts with beta-catenin, GSK-3beta and APC and reduces the beta-catenin level. Genes Cells 1998: 3: 395–403.
20. Maatouk DM, DiNapoli L, Alvers A et al. Stabilization of beta-catenin in XY gonads causes male-to-female sex-reversal. Hum Mol Genet 2008: 17: 2949–2955.
21. Gallagher ED, Gutowski S, Sternweis PC et al. RhoA binds to the amino terminus of MEKK1 and regulates its kinase activity. J Biol Chem 2004: 279: 1872–1877.
22. Tew SR, Hardingham TE. Regulation of SOX9 mRNA in human articular chondrocytes involving p38 MAPK activation and mRNA stabilization. J Biol Chem 2006: 281: 39471–39479.
23. Woods A, Wang G, Beier F. RhoA/ROCK signaling regulates Sox9 expression and actin organization during chondrogenesis. J Biol Chem 2005: 280: 11626–11634.
24. Kumar D, Lassar AB. The transcriptional activity of Sox9 in chondrocytes is regulated by RhoA signaling and actin polymerization. Mol Cell Biol 2009: 29: 4262–4273.
25. Murakami S, Kan M, McKeehan WL et al. Up-regulation of the chondrogenic Sox9 gene by fibroblast growth factors is mediated by the mitogen-activated protein kinase pathway. Proc Natl Acad Sci U S A 2000: 97: 1113–1118.
26. Cool J, Capel B. Mixed signals: development of the testis. Semin Reprod Med 2009: 27: 5–13.
27. Deswal S, Schulze AK, Hofer T et al. Quantitative analysis of protein phosphorylations and interactions by multi-colour IP-FCM as an input for kinetic modelling of signalling networks. PloS One 2011: 6: e22928.
28. Chow S, Patel H, Hedley DW. Measurement of MAP kinase activation by flow cytometry using phospho-specific antibodies to MEK and ERK: potential for pharmacodynamic monitoring of signal transduction inhibitors. Cytometry 2001: 46: 72–78.

Figure S1

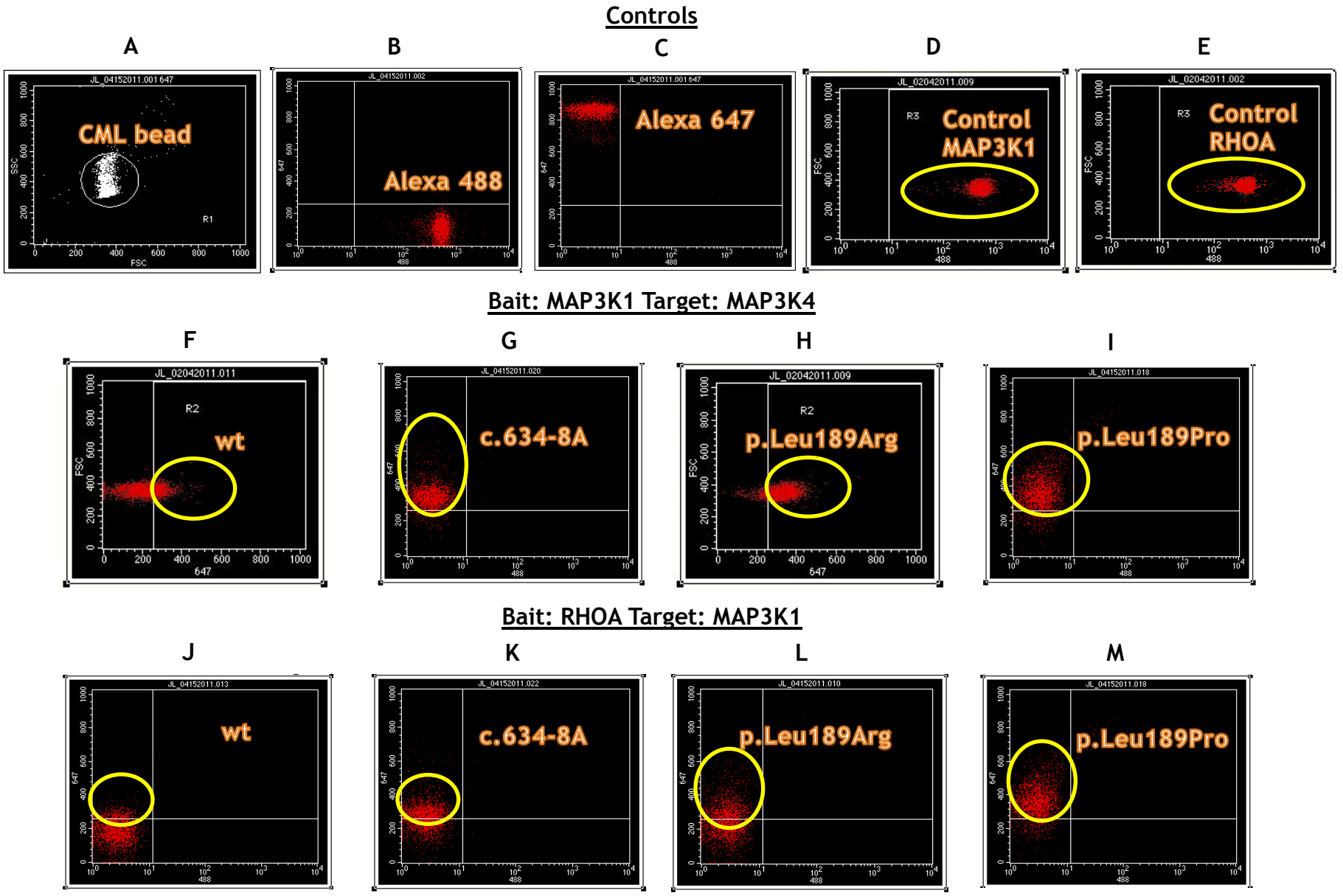
Controls
A
B
C
D
E
CML bead
Alexa 488
Alexa 647
Control MAP3K1
Control RHOA
Bait: MAP3K1 Target: MAP3K4
F
G
H
I
wt
c.634-8A
p.Leu189Arg
p.Leu189Pro
Bait: RHOA Target: MAP3K1
J
K
L
M
wt
c.634-8A
p.Leu189Arg
p.Leu189Pro

Figure S2

Controls

A

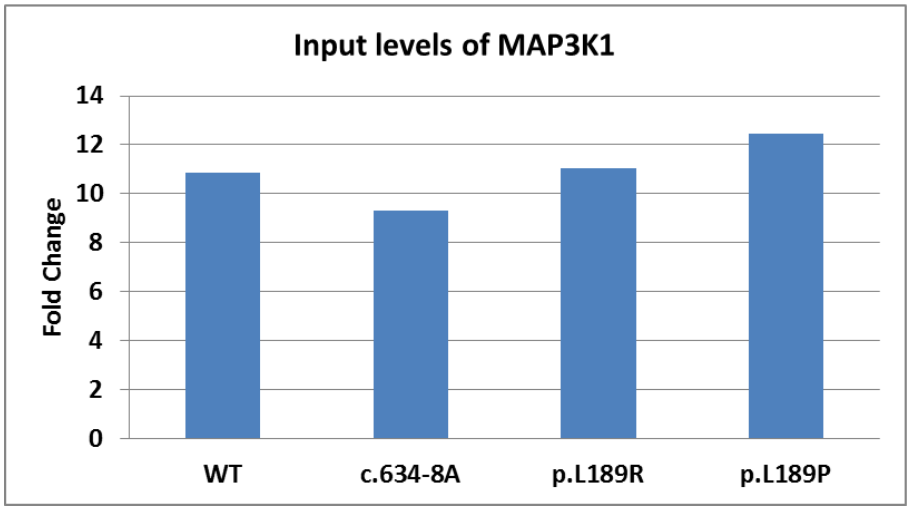

B

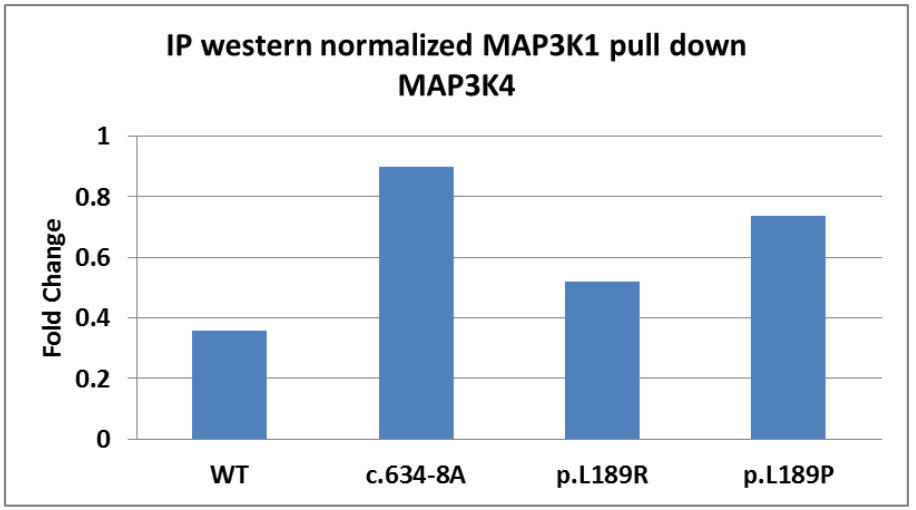

C